Time-Resolved Spectroscopy of Energy and Electron Transfer Processes in the Photosynthetic Bacterium *Heliobacillus mobilis*

Su Lin, Hung-Cheng Chiou, Frank A. M. Kleinherenbrink, and Robert E. Blankenship
Department of Chemistry and Biochemistry, Center for the Study of Early Events in Photosynthesis, Arizona State University, Tempe, Arizona 85287–1604 USA

ABSTRACT The kinetics of excitation energy transfer and electron transfer processes within the membrane of *Heliobacillus mobilis* were investigated using femtosecond transient absorption difference spectroscopy at room temperature. The kinetics in the 725- to 865-nm region, upon excitation at 590 and 670 nm, were fit using global analysis. The fits returned three kinetic components with lifetimes of 1–2 ps and 27–30 ps, and a component that does not decay within several nanoseconds. The 1- to 2-ps component is attributed to excitation equilibration to form a thermally relaxed excited state. The 27- to 30-ps phase corresponds to the decay of the relaxed excited state to form a charge-separated state. The intrinsic energy and electron transfer rates were estimated using the experimental results and theoretical models for excitation migration and trapping dynamics. Taking into account the number of antenna pigments and their spectral distribution, an upper limit of 1.2 ps for the intrinsic time constant for charge separation in the reaction center is calculated. This upper limit corresponds with the trapping-limited case for excitation migration and trapping. Reduction of the primary electron acceptor A_0 was observed in the 640 to 700 nm region using excitation at 780 nm. An instantaneous absorbance increase followed by a decay of about 30 ps was observed over a broad wavelength region due to the excited state absorption and decay of BChl *g* molecules in the antenna. In addition, a narrow bleaching band centered at 670 nm grows in with an apparent time constant of about 10 ps, superimposed on the 30-ps absorbance increase due to excited state absorption. Measurements on a longer time scale showed that besides the 670 nm pigment a BChl *g* molecule absorbing near 785 nm may be involved in the primary charge separation, and that this pigment may be in equilibrium with the 670 nm pigment. The bleaching bands at 670 nm and 785 nm recovered with a time constant of about 600 ps, due to forward electron transport to a secondary electron acceptor. Energy and electron transfer properties of *H. mobilis* membranes are compared with Photosystem I, to which the heliobacteria bear an evolutionary relationship.

INTRODUCTION

The primary processes of energy transfer and charge separation in photosynthetic systems have been studied extensively by various spectroscopic methods, in particular ultrafast time-resolved spectroscopy (Sundström and van Grondelle, 1991). However, a detailed understanding of antenna processes and how they are coupled to electron transfer in photosynthetic reaction centers is still lacking.

The heliobacteria are a newly discovered group of non-oxygen evolving photosynthetic bacteria (Gest and Favinger, 1983; Beer-Romero and Gest, 1987; Madigan, 1992). This family of organisms has a photosynthetic apparatus with a very simple structure, in that the antenna and reaction center are organized as a single pigment-protein complex with approximately 35–40 antenna molecules per reaction center, with bacteriochlorophyll (BChl) *g* as the major pigment (Nuijs et al., 1985; Trost and Blankenship, 1989; Vos et al., 1989; Van de Meent et al., 1990). Recent evidence indicates that the heliobacteria probably contain a homodimeric core protein complex (Liebl et al., 1993). This is in contrast to the heterodimeric protein complexes found in most other photosynthetic reaction centers. This combination of properties suggests that the heliobacteria are the most primitive photosynthetic organisms yet examined.

The reaction center of the heliobacteria is broadly similar to that of Photosystem I of oxygen evolving organisms (Prince et al., 1985; Trost and Blankenship, 1989; Vos et al., 1989; Van de Meent et al., 1990; Nitschke et al., 1990a; Trost et al. 1992). Similar findings have also linked the reaction center of green sulfur bacteria to Photosystem I (Prince and Olson, 1976; Nitschke et al., 1990b; Büttner et al., 1992). These organisms may be considered as bacterial models for Photosystem I in the same way that purple bacteria are used as models for Photosystem II (Michel and Deisenhofer, 1988). The BChl *g* antenna in the heliobacteria contains at least three different spectral forms that can be distinguished at low temperatures, named BChl *g* 778, BChl *g* 793, and BChl *g* 808, respectively (Van Dorssen et al., 1985; Smit et al., 1989). Absorption, fluorescence emission and excitation measurements at room and low temperature have indicated that efficient energy transfer takes place from the higher energy species BChl *g* 778 and BChl *g* 793 to the lower energy BChl *g* 808 and from BChl *g* 808 to the primary electron donor P798 (Van Dorssen et al., 1985; Smit et al., 1989; Van Kan et al., 1989; Kleinherenbrink et al., 1992). Recent kinetic studies have suggested that the processes of excitation energy transfer within the antenna system and from the antenna to the reaction center take place on a picosecond time scale (Trost and Blankenship, 1989; Van Noort et al., 1992).

Received for publication 30 August 1993 and in final form 10 November 1993.

Address reprint requests to Dr. Robert E. Blankenship, Department of Chemistry and Biochemistry, Arizona State University, Tempe, AZ 85287-1604. Tel.: 602-965-1439; Fax: 602-965-2747; E-mail: blankenship@asuchm.la.asu.edu.

0006-3495/94/02/437/09 $2.00

In order to obtain detailed direct information about the excitation distribution within the antenna and transfer to the reaction center and about the initial charge separation processes within the reaction center of heliobacteria, we have studied membranes of *Heliobacillus mobilis* (*H. mobilis*) by using femtosecond transient absorption spectroscopy.

MATERIALS AND METHODS

H. mobilis was grown anaerobically in a 13-liter bottle for 36 h at 37°C under 500 W of incandescent illumination from a 1-liter inoculum in Medium 112 (Gest and Favinger, 1983) plus 20 mM sodium pyruvate. Cells were harvested by continuous flow centrifugation and washed once with 20 mM Tris-5 mM sodium ascorbate, pH 8.0, buffer. All buffers used were thoroughly degassed and stored under nitrogen. Membranes were isolated as described earlier (Trost and Blankenship, 1989) by sonication and centrifugation at 10,000 × *g* for 10 min, followed by ultracentrifugation of the supernatant liquid at 200,000 × *g* for 2 h. The pelleted membranes were resuspended in buffer to an absorbance above 150 at 788 nm.

For femtosecond transient absorption measurements, the stock membranes were diluted in a buffer solution with 25 mM Tris, pH 8.0, 20 mM ascorbate, and 100 μM phenazine methosulfate (PMS). For some experiments, the secondary electron acceptors were reduced using a buffer solution with 100 mM glycine, pH 11.0, 20 mM ascorbate, 100 μM PMS, and 50 mM sodium dithionite. Samples were loaded in a spinning cell with an optical path length of 2.5 mm and a diameter of 18 cm. The absorbance of the samples varied between 1.5 and 2.3 at 788 nm (2.5 mm path) depending on the type of measurement. The sample cell was rotated at two revolutions per second to ensure that a fresh area was exposed for each laser flash. The excitation intensity was adjusted such that for each excitation pulse less than 0.25 photon was absorbed per reaction center. The number of photons absorbed by each reaction center per laser pulse was calculated (Cho et al., 1984) using the measured pulse energy of 1.85 μJ per pulse focused on a 2-mm spot in the sample, and the estimated optical cross section of reaction center at 590 nm, of 1.33×10^{-15} cm^2. This was calculated using an assumed extinction coefficient at 590 nm of 10^4 liter Mol^{-1} cm^{-1} along with a photosynthetic unit size of 35 BChl *g* per reaction center (Trost and Blankenship, 1989; Van de Meent et al.; 1990). Control experiments at variable pump intensities confirmed that the magnitude of the absorbance change observed was directly proportional to and the kinetics were independent of the pump intensity.

The laser pulse train used in the femtosecond spectral measurements was provided by a single jet ultrashort pulse dye laser (Spectra-Physics Model 3500) synchronously pumped by a frequency-doubled, mode-locked cw Nd:YAG laser (Spectra Physics Model 3800). Both laser pulse trains were compressed using fiber compression techniques (Spectra-Physics Model CP1 and Model 3695 pulse compressors). The laser pulse was then amplified by a three-stage picosecond tunable dye amplifier (Continuum Model PTA1000) pumped by a high repetition rate regenerative amplifier (Continuum Model RGA1000). The final output optical pulses from the laser and amplifier system were 200 fs full width at half maximum at 590 nm, 200 μJ, at a repetition rate of 540 Hz (Taguchi et al., 1992).

The laser beam was split into a pump and probe beam, and the probe beam was rotated 54.7° with respect to the polarization of the pump beam. The pump beam was focused into the sample directly for the 590 nm excitation measurements. For the 780- or 670-nm excitation, the pump beam was focused into a 1-cm water flow cell to generate a white light continuum and sent through a 10-nm band pass filter centered at 780 or 670 nm. The beam was reamplified by a prism amplifier pumped by a 532-nm beam from the regenerative amplifier.

The probe beam was split into two identical parts, as the probe and the reference beams, respectively. A variable time delay of the probe and reference beam relative to the pump beam was provided by a computer controlled translation stage. The probe and the reference signals were focused onto two separate optical fibers coupled to a monochromator (Acton Research Corporation model Spectra Pro 275). The spectra were acquired on a dual array optical multichannel analyzer (Princeton Instruments models DPAA-1024 and ST121) at 0.14 nm per channel and were averaged over 10^4 laser shots at each time delay.

Data analysis was performed using locally written software. Decay associated spectra (DAS) were obtained by fitting transient absorption change curves over a selected wavelength region simultaneously using Eq. 1

$$\Delta OD(\lambda, t) = \sum_{i=1}^{n} A_i(\lambda)\exp(-t/\tau i) \quad (1)$$

where ΔOD (λ, t) is the observed absorption change at a given wavelength (λ) and time delay (t); n is the number of kinetic components used in the fitting; a plot of $A_i(\lambda)$ versus wavelength is called a decay associated spectrum, which represents the amplitude spectrum of the ith kinetic component, which has a decay lifetime of τ_i.

RESULTS

Q_y band of BChl *g*, excitation at 590 nm

Transient absorption difference spectra of membranes of *H. mobilis* were measured in the 725 to 865 nm Q_y band region at room temperature upon excitation at 590 nm. The excitation wavelength is near the Q_x transition band of BChl *g*. At this wavelength, most photons are absorbed by antenna pigments. Excitation annihilation processes in the antenna were judged to be negligible, based both on a calculation of the expected number of photons absorbed per reaction center and the observed independence of the observed kinetics to changes of a factor of two of light intensity (see Materials and Methods).

Fig. 1 *A* shows the time-resolved spectra at early times

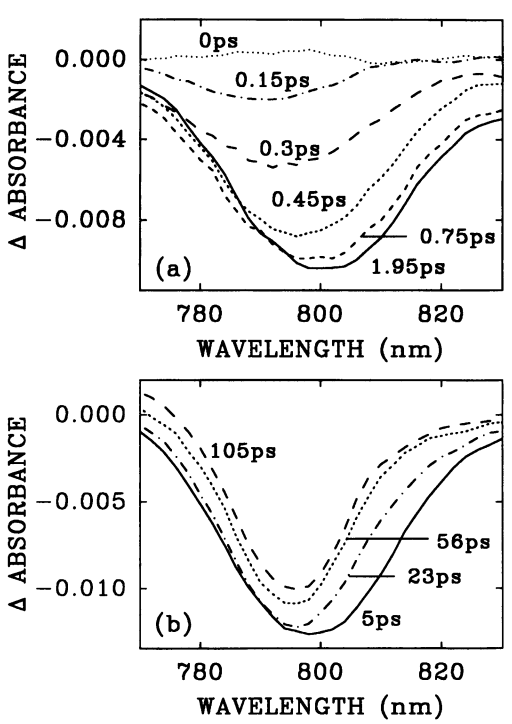

FIGURE 1 Time-resolved absorbance difference spectra of membranes of *H. mobilis* at room temperature after laser excitation at 590 nm at (*A*) 0 ps, 0.15 ps, 0.3 ps, 0.45 ps, 0.75 ps, and 1.95 ps, and (*B*) 5 ps, 23 ps, 56 ps, and 105 ps.

(0–2 ps). A photobleaching band developed initially around 794 nm during the first 0.45 ps and shifted to longer wavelengths at later times. The spectral shift was completed within 2 ps and ended around 802 nm. It is probably due to the redistribution of excitations among different spectral forms of BChl *g*, with a possible contribution from intramolecular relaxation processes from upper excited states to the thermally equilibrated lowest excited state. The time-resolved spectra at later times (5, 23, 56, and 105 ps, in Fig. 1 *B*) show that the amplitude of the bleaching band decreased and the peak shifted back to the blue. The maximum bleaching was located at 798 nm at 105 ps and did not change at later times. This band (100 ps and later) is due to the formation of $P798^+$, the oxidized primary electron donor (Fuller et al., 1985; Nuijs, et al., 1985; Prince et al., 1985; Trost and Blankenship, 1989; Nitschke et al., 1990a).

Transient absorption difference kinetics taken on a 150-ps time scale in the wavelength range of 770–830 nm were fitted using global analysis. The results are shown in Fig. 2. The decay profiles at three BChl *g* absorption wavelengths 778, 793, and 808 nm are illustrated in Fig 2 *A*. Two kinetic components (0.7 ps and 26.8 ps) and a constant are needed to fit the decay profiles adequately in the entire wavelength region. The smooth lines in Fig. 2 *A* are the fitting results at the corresponding wavelengths. The decay associated spectra of the three kinetic components are shown in Fig. 2 *B*. The long-lived component is a photobleaching signal centered at 798 nm that represents the oxidized primary donor $P798^+$. Its spectral shape is very similar to the difference spectrum measured at 105 ps after excitation (Fig. 1). The 0.7-ps component has negative amplitude below 776 nm and a positive amplitude at longer wavelengths (global analysis on data sets with 0.15 ps time resolution also show this 1–2 ps rise component). The 26.8-ps decay component shows the recovery of a band peaking at 808 nm with a shoulder extending to 780 nm. The average time constant for this component obtained from various data sets and fits is 28 ± 5 ps. This is in good agreement with measurements of fluorescence decay kinetics, which gave a value of 25 ps (Trost and Blankenship, 1989). A similar decay time was also recently observed in picosecond transient absorption experiments by van Noort et al. (1992).

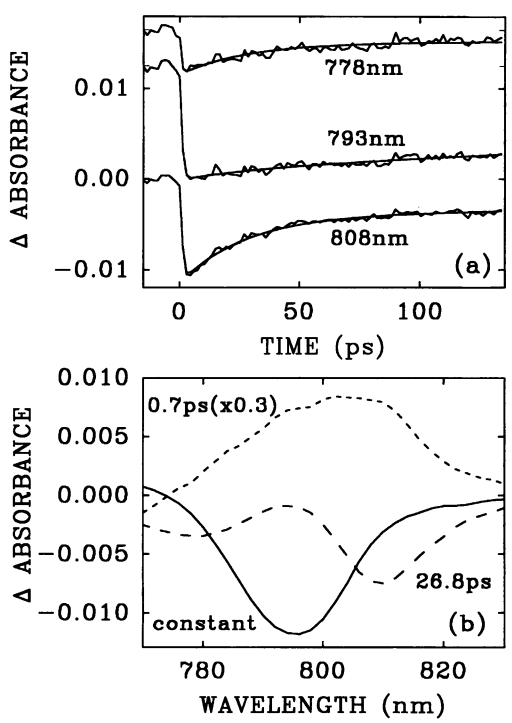

FIGURE 2 Kinetics and global analysis of absorption difference spectra of membranes of *H. mobilis* at room temperature with 590 nm laser excitation. (*A*) Decay profiles at 778 nm (upper), 793 nm (middle), and 808 nm (lower) with theoretical fittings at corresponding wavelengths (smooth lines). (*B*) Decay associated spectra from the fit with three kinetic components: 0.7 ps (short dashed line, reduced by a factor of 2), 26.8 ps (long dashed line) and constant (solid line).

Q_y band of BChl *g*, excitation at 670 nm

Kinetics in the same wavelength region were also examined by exciting samples at 670 nm. At this wavelength, as much as 50% of the absorption is due to pigments with maximum Q_y absorption at 670 nm, one of which functions as the primary electron acceptor A_0 (Nuijs et al., 1985; Van Kan et al., 1989; Van de Meent et al., 1991). The time-resolved spectra at early times are broadly similar to those upon excitation of the antenna at 590 nm, showing a broad bleaching centered around 795 nm that shifts to 802 nm within 1–2 ps. The spectra taken at later times show a decrease of the bleaching and the band shifted back to the blue. The spectrum taken at 100 ps and later is centered at 798 nm and represents the oxidized primary donor $P798^+$.

Global analysis of the transient absorbance change in the wavelength region 770 to 830 nm results in three kinetic components shown in Fig. 3. A fast component with a time constant of 0.7 ps, similar to the 0.7-ps component in Fig. 2, is once again observed. The middle component shows a bleaching band centered at 810 nm. The lifetime of this component is found to be 27 ± 4 ps from various data sets. We may assume that it reflects the same process as the 28-ps

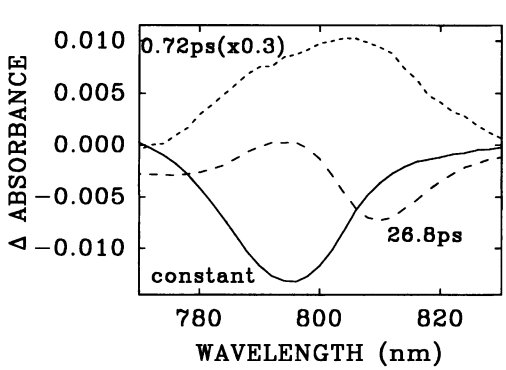

FIGURE 3 Decay-associated spectra obtained from a three component global fit of the transient absorption kinetics upon excitation at 670 nm. The medium-dashed line, the long-dashed line and the solid line represent decay components of 0.72 ps, 26.8 ps and a constant, respectively.

component upon excitation at 590 nm (Fig. 1), i.e., energy transfer from the antenna to P798 and subsequent charge separation. The long-lived component is ascribed to the charge separated state $P798^+$.

Q_y band of the primary acceptor A_0, excitation at 780 nm

To obtain direct information about the formation of the primary charge separated state, kinetics were measured in the 670 nm band where the primary electron acceptor A_0, 8^1-hydroxy Chl *a* (Van de Meent et al., 1991), absorbs. Absorbance difference spectra in the 640 to 700 nm region were measured upon excitation at 780 nm, in the Q_y transition band of BChl *g* (Fig. 4 *A*). An instantaneous absorbance increase followed by a decay was observed over a broad wavelength region. In addition, a narrow bleaching band peaking at 670 nm developed. The instantaneous rise of the absorption is due to excited state absorption of the antenna when its Q_y band was directly excited. The 670 nm bleaching has been assigned to the formation of A_0^- (5, 19). A Chl *a*-like breakdown product of BChl *g* also absorbs in this region (Beer-Romero et al., 1988) but is probably not associated with functional reaction centers. It cannot be excited directly with 780 nm excitation.

Global analysis over the 640–700 nm wavelength region gave three exponential components: a fast decay of 1.5–3 ps, an intermediate decay of 29 ps, and a slow bleaching recovery that was determined to have a time constant of about 600 ps in a longer timescale measurement (see below). The decay-associated spectra of the three components are shown in Fig. 4 *B*. The long-lived component represents the bleaching due to the reduced primary electron acceptor A_0^-. The 30-ps lifetime is the same as that of the antenna and agrees with the kinetics observed by van Noort et al. (1992). An analysis of the same data set, in which just the amplitude of the 670 bleaching was plotted against time (after correction at each time point for the broad absorbance increase due to excited antenna BChl *g*) yielded a formation time of about 10 ps for the A_0^- bleaching, as shown in Fig. 4 *C*. Also shown in Fig. 4 *C* is a theoretical fit to the 670 nm absorbance change data. The theoretical fit involves an equilibrium between the 670 nm absorbing primary acceptor species (B) and another species, C. The possible identity of C is considered in the Discussion.

Spectra measured on nanosecond time scale

Absorption difference spectra in the 670-nm and 800-nm regions were also measured on a nanosecond timescale upon excitation at 780 nm and 590 nm, respectively. Fig. 5 *A* shows the difference spectrum in the 670-nm region upon 780-nm excitation, taken at 140 ps minus that taken at 2 ns. The spectrum shows a narrow bleaching band centered at 670 nm, which is due to the formation and decay of A_0^- (see above). The recovery of the 670-nm band shown in Fig. 5 *C* was fit with one exponential decay of 594 ps plus a constant.

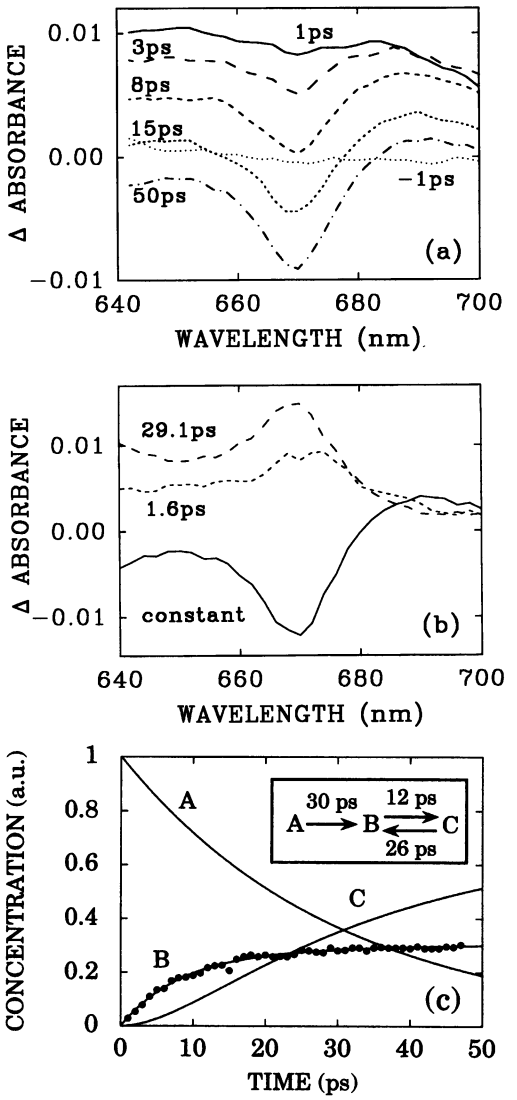

FIGURE 4 (*A*) Time-resolved spectra in the 670 nm region with 780 nm excitation, at −1 ps, 1 ps, 3 ps, 8 ps, 15 ps, and 50 ps. (*B*) Decay associated spectra from a three-component fitting. (*C*) Solid circles: Amplitude of the 670 nm bleaching band as a function of time, as obtained after subtraction of the broad absorbance increase across this spectral region. The data obtained in this way represent the transient population of the reduced primary acceptor A_0. The drawn curves represent the result of a fit using a simple kinetic model (see inset) with three states (A, B, and C), involving an irreversible process (A → B) with a time constant of 30 ps and a reversible process (B → C). The curve through the data points represents the transient population of state B, with the concentrations of A = 1 and B = C = 0 at $t = 0$. The time constant for step (A → B) was kept fixed at 30 ps to represent the trapping of antenna excitations to form the charge separated state. The time constants for the reversible reaction (B → C) were obtained from a fit of the transient population of the reduced primary acceptor A_0 using the equation for the transient population of B as given in Moore and Pearson (1981) for this kinetic model.

A similar result was obtained by Nuijs et al. (1985) for *H. chlorum* in the same wavelength region, and ascribed to reoxidation of A_0^- due to forward electron transport.

Upon addition of dithionite at high pH, the absorption difference spectra at 100 ps and 2 ns were virtually identical (Fig. 6 *A*). Under these conditions forward electron transport

is inhibited and charge recombination between $P798^+$ and A_0^- takes 17 ns (Kleinherenbrink et al., 1991). Fig. 6 *B* shows spectra at 100 ps and 2 ns for a sample without dithionite. The bleaching at 670 nm is completely developed by 100 ps and has largely decayed by 2 ns. The rise time of the 670 nm band was identical to that in the absence of dithionite (Fig. 4), which may indicate that the rate of charge separation in the reaction center is not affected by reduction of the secondary acceptor(s) (see Discussion).

Absorption changes are also observed on the nanosecond timescale in the 800-nm region (Nuijs et al., 1985). Fig. 5 *B* shows the subtraction of spectra taken at 150 ps and 2 ns (inset), upon 590-nm excitation, which gives a bleaching around 785 nm. The time trace at 790 nm shown in Fig. 5 *D* was obtained by taking the difference between decays at 790 nm and 800 nm in order to separate the kinetics of the 785-nm band from the main bleaching band of $P798^+$. These kinetics could be adequately fitted with a time constant of 610 ps, suggesting that they reflect the same process sampled at 670 nm (see above). The absorption difference spectrum in Fig. 5 *B* shows the recovery of a BChl *g* bleaching around 785 nm and clearly not a BChl *g* bandshift, as has been suggested earlier (Kleinherenbrink et al., 1991). It decays with the same kinetics as the 670-nm band when the electron is transferred from A_0 to a secondary electron acceptor.

DISCUSSION

Estimation of the charge separation rate in the reaction center

Our measurements on membranes of *H. mobilis* give a global view of the spectral changes and kinetics at early times after laser excitation. The decay of excitations in the equilibrated antenna of *H. mobilis* due to trapping in the reaction center was found to have a time constant of about 30 ps. Equilibration of excitations over the different spectral forms of BChl *g* in the antenna occurred within 1–2 ps, indicating that energy transfer between neighboring pigment molecules is a subpicosecond process. If the rates of energy transfer between the reaction center and neighboring antenna molecules are equally fast, and if the number of nearest neighbors is the same for antenna and reaction center pigments, the probabilities for excitations to be on any of the pigments (including the reaction center) are the same. This would result in an excitation lifetime

$$\tau_{ex} = N\,\tau_{cs} \tag{2}$$

where τ_{cs} is the time constant for the charge separation process ($P^*A_0 \rightarrow P^+A_0^-$) in the reaction center, and N is the total number of pigment molecules per reaction center. Assuming $N = 35$ (Trost and Blankenship, 1989; Van de Meent et al., 1990), this would yield a time constant for charge separation $\tau_{cs} \approx 0.9$ ps. However, the effective number of antenna pigments per reaction center is probably lower than 35, since spectral equilibration accumulates excitations mainly on BChl *g* 793 and BChl *g* 808, i.e., the low energy pools of antenna BChl *g*. Furthermore, we should take into account the fact that the primary electron donor P798 absorbs at considerably shorter wavelength than BChl *g* 808. This results in an expression of the excitation lifetime (Trissl, 1993)

$$\tau_{ex} = N_{eff}\tau_{cs}\exp((E_{798} - E_{808})/kT) \tag{3}$$

where k is Boltzmann's constant, T is the absolute temperature and a value for the effective number of antenna pigments, N_{eff}, may be calculated using the equation

$$N_{eff} = \sum_i N_i \exp(-(E_i - E_{808})/kT) \tag{4}$$

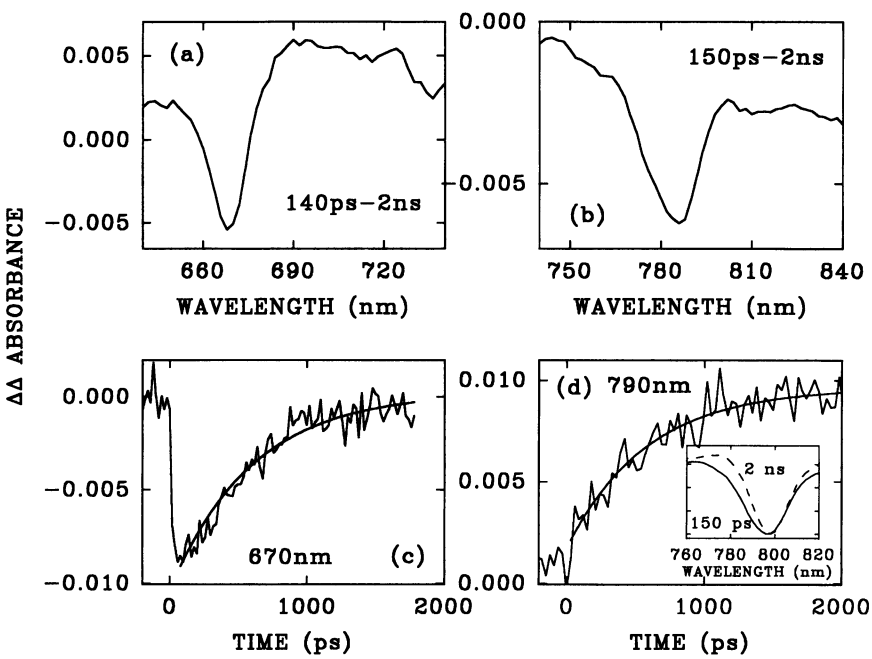

FIGURE 5 Absorbance difference difference spectra constructed from the spectra taken at (*A*) 140 ps minus 2 ns using 780 nm excitation and (*B*) 150 ps minus 2 ns using 590 nm excitation. (*C*) Kinetics at 670 nm with a time resolution of 20 ps per channel. The smooth curve is the theoretical fit with an exponential decay of 594 ps and a constant. (*D*) Kinetics at 790 nm with a time resolution of 30 ps per channel. The curve is obtained by taking the difference between the decay at 800 nm and the decay at 790 nm (see text). The smooth curve is a theoretical fit with an exponential time constant of 610 ps plus a constant. Inset: time resolved spectra taken at 150 ps (solid line) and 2 ns (dashed line) after the laser flash.

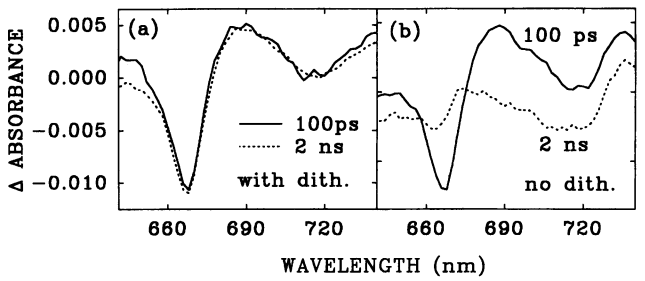

FIGURE 6 Time-resolved absorbance difference spectra of membranes of *H. mobilis* at room temperature at 100 ps (solid line) and 2 ns (dashed line) after laser excitation at 780 nm. (*A*) Sample with 50 mM dithionite added; (*B*) Sample with no additions.

The number of BChls in each of the 778-, 793-, and 808-nm antenna pools, N_i, can be found from the deconvolution of the low temperature absorption spectrum of *Heliobacterium chlorum* (Smit et al., 1989). The energies E_i for each antenna pool and the primary donor in Eqs. 3 and 4 can be calculated from the wavelength of their maximum absorption. In this way a value $N_{eff} \approx 12$ was obtained from Eq. 4, yielding $\tau_{cs} \approx 1.2$ ps from Eq. 3.

The above assumption of relatively fast energy transfer among all pigment molecules and relatively slow charge separation in the reaction center corresponds to the so-called "trapping-limited" case, where an excitation visits the site of the reaction center many times before it is trapped by photochemistry (Pearlstein, 1982, 1984). However, it is not yet certain that this situation indeed applies to the heliobacterial antenna-reaction center complex. Although the antenna and photoactive pigments are associated with the same peptide, the distance between the photoactive pigments and neighboring antenna pigments might be larger than between neighboring antenna pigments. Even a small increase in this distance could result in a significant decrease in the corresponding energy transfer rate. Furthermore, energy transfer from the bulk antenna to the reaction center is thought to occur through BChl *g* 808, and the overlap between BChl *g* 808 emission and P798 absorption (which is proportional to the energy transfer rate) might well be considerably smaller than vice versa. Therefore, it is possible that the energy transfer step from the antenna pigments to the photoactive pigments is considerably slower than hopping between neighboring antenna molecules. Such a situation would correspond to a "special trapping-limited" case (Sundström and van Grondelle, 1990; Otte et al., 1993), in which not charge separation itself, but the final energy transfer step into the reaction center is the rate limiting process. Recently, the very low escape probability to the antenna for excitations on the reaction center of purple bacteria was explained by a similar reasoning (Otte et al., 1993).

Transient absorption kinetics upon direct excitation of reaction center pigments should in principle allow us to determine whether an excitation can escape from the reaction center to the antenna. This would then allow us to distinguish between the trapping-limited case (high escape probability) or the "special trapping-limited" case (low escape probability). Our decay associated spectra upon direct excitation of the primary acceptor at 670 nm (Fig. 3) show considerable similarity between the spectral shape and relative amplitude of the 30 ps decay component compared with that upon excitation at 590 nm (Fig. 2), which would indicate a very high escape probability for reaction center excitations. However, the major part of the absorption at 670 nm is still due to antenna pigments and degradation products (Beer-Romero et al., 1988), making it difficult to accurately determine the escape probability from the present data.

The above considerations make it useful to describe energy transfer and charge separation in terms of a model developed by Pearlstein (1982; 1984). In this model, the antenna-reaction center complex is described as a regular lattice of equidistant pigments. Under conditions where only the antenna is excited and energy transfer between antenna pigments is very fast, the model predicts an overall excitation lifetime

$$\tau_{ex} = (qF_t)^{-1}N + \tau_{cs}\,(1 + (N - 1)\,I_d/I_t) \qquad (5)$$

in which q is the number of nearest neighbors to the photoactive pigments (the coordination number, with a likely value from 1 to 6), F_t is the energy transfer rate to the photoactive pigments from a neighboring antenna pigment, and I_d and I_t are the overlap factors between the photoactive pigment's emission and the nearest neighbor's absorption and vice versa. The parameter N represents the number of pigments per reaction center, for which the effective value will be used, since the Pearlstein model does not account for spectral inhomogeneity. The term $(qF_t)^{-1}N$ represents the "first passage time," i.e., the average time needed for an excitation to reach the reaction center site for the first time. Taking typical values of N_{eff} of 10–40 (Trissl, 1993) and assuming that the rate of energy transfer to the reaction center from neighboring pigments F_t is very high, $(0.1\ \text{ps})^{-1}$, the first passage time becomes negligible and Eq. 5 reduces to Eq. 3, the trapping-limited case. It becomes clear from Eq. 5 that the charge separation time τ_{cs} cannot be larger than the 1.2 ps found above for the trapping-limited case, which may thus be taken as an upper limit. This means that the room temperature charge separation rate in the reaction center of heliobacteria might be faster than that in purple bacteria, which is found to be about 3 ps in several species (Kirmaier and Holten, 1987). Because information about the values of F_t and q in Eq. 5 is lacking, a lower limit for the charge separation time cannot be given.

The primary charge separated state

The 670-nm bleaching band that appears upon excitation in the Q_y band of BChl *g* (Fig. 3) originates from the formation of A_0^-(8^1-hydroxy Chl *a* (van de Meent et al., 1991)), consistent with the results of earlier measurements (Nuijs, et al., 1985; Van Noort et al., 1992). The 30-ps component result-

ing from global analysis of the kinetics in this region (Fig. 4) is consistent with the overall decay lifetime of the antenna (Trost and Blankenship, 1989). However, there also appears to be a faster phase to the decay in this region. This is shown in Fig 4 *B* as a 1.6-ps phase in a global analysis of the data in this wavelength region, and in Fig. 4 *C* as a 10-ps phase in the data measured at 670 nm, after subtraction of the broad absorbance increase across the region. Single wavelength fits across the 670-nm band returned faster decay constants in the center of the band than on the wings (data not shown). One possible mechanistic explanation for the behavior at 670 nm is illustrated in Fig. 4 *C*. If the reduced primary electron acceptor reaches an equilibrium with another species, the apparent time constant of its formation may be faster than the 30-ps rate constant of the process that forms the charge separated state. The similarity of the kinetics at 670 nm and 785 nm measured on the nanosecond time scale (Fig. 5) suggests that there are two decaying bleaching bands that reflect electron transfer from the primary electron acceptor to the next electron acceptor. One possibility is that the equilibrium indicated by the fit in Fig. 4 *C* is between the primary electron acceptor and the 785-nm absorbing pigment. Additional experiments are underway to test this idea.

The spectral shape of the 785-nm band (Fig. 5) indicates that it is not likely to be due to an electrochromic shift of BChl *g*, as has been suggested earlier (Kleinherenbrink et al., 1991), in that the characteristic derivative shape of a spectral bandshift is not observed. The absorbance changes appear to be a simple bleaching of a spectral form of BChl *g* that absorbs around 785 nm. Both bands in Figs. 5 *A* and 5 *B* are associated with the primary charge separated state, which indicates that besides A_0 (8^1-hydroxy Chl *a* (Van de Meent et al., 1991)), a BChl *g* molecule might also be reduced in the primary charge separation, or is very closely coupled to the 670-nm pigment. Further research is currently underway to investigate this point.

Comparison with Photosystem I

Because the heliobacteria have an evolutionary relationship with Photosystem I (Prince et al., 1985; Trost and Blankenship, 1989; Vos et al., 1989; Nitschke et al., 1990a; Van de Meent et al., 1990; Trost et al., 1992; Liebl et al., 1993), it is of interest to compare our results and the pathways and kinetics of energy and electron transfer in the two systems. There are numerous spectroscopic studies of excitation energy transfer and electron transfer processes in Photosystem I with a variety of preparations containing chlorophyll to P700 (the primary electron donor in Photosystem I) ratios ranging from 10–200 (for reviews see Sètif, 1992; Golbeck and Bryant, 1991). As in heliobacteria, the presence of antenna pigments makes it difficult to study the energy transfer and electron transfer processes independently.

In order to determine the charge separation rate from the observed decay time of antenna excitations after equilibration, assumptions have to be made about the mechanism of energy transfer and trapping. Several authors have concluded that the rate of excitation trapping in Photosystem I is limited by charge separation, on the basis of the relatively long overall trapping times compared with the energy transfer time between antenna pigments (Owens et al., 1987; Turconi et al., 1993; Holzwarth et al., 1993), and references therein. Assuming trapping limited kinetics and using a spectral decomposition method to calculate the effective antenna size, Trissl et al. (1993) calculated a value of 2.3 ps for the charge separation time in Photosystem I, i.e., slightly longer than the value upper limit of 1.2 ps that we propose for heliobacteria. A similar value has been estimated by Owens et al. (1987), who concluded, however, that the kinetics were essentially diffusion limited. Although the "special trapping-limited" case (Sundstrom and van Grondelle, 1990; Otte et al., 1993) has not been considered for excitation transfer and trapping in Photosystem I (Owens et al., 1987; Turconi et al., 1993; Holzwarth et al., 1993; Trissl et al., 1993), it should probably not be ruled out as a possibility.

In Photosystem I, the acceptor A_0 that is reduced in the primary charge separation is a Chl *a* species absorbing around 685–690 nm (Golbeck and Bryant, 1991). No involvement of any other pigment besides P700 and A_0 in the primary charge separation has been reported, but a shoulder at 670 nm has sometimes been observed in the A_0^- difference spectrum (Shuvalov et al., 1986; Golbeck and Bryant, 1991). In this respect it may be interesting to note that the crystal structure of the Photosystem I core, that has recently been published (Krauss et al., 1993), indicated the possible presence of an accessory pigment between P700 and A_0.

Forward electron transfer from A_0 to the secondary electron acceptor A_1 (phylloquinone) is thought to be exceptionally fast in Photosystem I, with a time constant of 32 ps (Shuvalov et al., 1986) or 21 ps (Hastings et al., 1994). In *H. mobilis*, forward electron transfer from A_0 was found to occur with a much slower time of 600 ps, indicating that the next electron acceptor might be different than in Photo system I. Currently, there is contradictory evidence whether a quinone functions as acceptor A_1 in heliobacteria (Trost et al., 1992; Kleinherenbrink et al., 1993).

The heliobacteria probably contain a homodimeric protein core for the reaction center, consisting of two identical copies of a single peptide (Leibl et al., 1993), whereas Photosystem I contains a heterodimeric protein core (Golbeck and Bryant, 1991). Whether or not the heterodimeric Photosystem I reaction center proteins give rise to two potential pathways of electron transfer, with only one being active, as is found in purple bacteria, is uncertain, although this is widely assumed to be the case. The simplest extrapolation to the heliobacteria suggests that these organisms might contain two functional pathways of electron transfer, although the symmetry of a homodimeric complex could be broken by an asymmetric interaction with an additional subunit. The presence of integral antenna pigments in both the Photosystem I and heliobacterial complexes makes the question of pathways of electron transfer

difficult to answer, and a resolution of these important problems will require additional experiments using multiple techniques.

We thank Profs. R. van Grondelle and J. Amesz, and Drs. R. G. Alden and G. Hastings for very helpful discussions.
Funding for this research is from NSF grant DMB-9106685.
This is publication #170 from the Arizona State University Center for the Study of Early Events in Photosynthesis.

REFERENCES

Beer-Romero, P., and Gest, H. 1987. *Heliobacillus mobilis*, a peritrichously flagellated anoxyphototroph containing bacteriochlorophyll *g*. *FEMS Microbiol. Lett.* 41:109–114.

Beer-Romero, P., Favinger, J. L., and Gest, H. 1988. Distinctive properties of bacilliform photosynthetic heliobacteria. *FEMS Microbiol. Lett.* 49: 451–454.

Büttner, M., Xie, D. L., Nelson, H., Pinther, W., Hauska, G., and Nelson, N. 1992. Photosynthetic reaction center genes in green sulfur bacteria and in Photosystem 1 Are related. *Proc. Natl. Acad. Sci. (USA)*, 89:8135–8139.

Cho, H. M., Mancino, L. J., and Blankenship, R. E. 1984. Light saturation curves and quantum yields in reaction centers from photosynthetic bacteria. *Biophys. J.* 45:455–461.

Fuller, R. C., Sprague, S. G., Gest, H., and Blankenship, R. E. 1985. A unique photosynthetic reaction center from *Heliobacterium chlorum*. *FEBS Lett.* 182:345–349.

Gest, H., and Favinger, J. L. 1983. *Heliobacterium chlorum*, an anoxygenic brownish-green photosynthetic bacterium containing a "new" form of bacteriochlorophyll. *Arch. Microbiol.* 136:11–16.

Golbeck, J. H., and Bryant, D. A. 1991. Photosystem I. *Curr. Top. Bioenerg.* 16:83–177.

Hastings, G., F. A. M. Kleinherenbrink, S. Lin, T. McHugh and R. E. Blankenship. 1994. Observation of the reduction and re-oxidation of the primary electron acceptor in Photosystem I. *Biochemistry*. In press.

Holzwarth, A. R., Schatz, G., Brock, H., and Bittersmann, E. 1993. Energy transfer and charge separation kinetics in Photosystem I. 1. Picosecond transient absorption and fluorescence study of cyanobacterial Photosystem I particles. *Biophys. J.* 64:1813–1826.

Kirmaier, C., and Holten, D. 1987. Primary photochemistry of reaction centers from the photosynthetic purple bacteria. *Photosynth. Res.* 13: 225–260.

Kleinherenbrink, F. A. M., Aartsma, T. J., and Amesz, J. 1991. Charge separation and formation of bacteriochlorophyll triplets in *Heliobacterium chlorum*. *Biochim. Biophys. Acta* 1057:346–352.

Kleinherenbrink, F. A. M., Deinum, G., Otte, S. C. M., Hoff, A. J., and Amesz, J. 1992. Energy Transfer from Long-Wavelength Absorbing Antenna Bacteriochlorophylls to the Reaction Center. *Biochim. Biophys. Acta* 1099:175–181.

Kleinherenbrink, F. A. M., Ikegami, I., Hiraishi, A., Otte, S. C. M., and Amesz, J. 1993. Electron transfer in menaquinone-depleted membranes of *Heliobacterium chlorum*. *Biochim. Biophys. Acta* 1142:69–73.

Krauss, N., Hinrichs, W., Witt, I., Fromme, P., Pritzkow, W., Dauter, Z., Betzel, C., Wilson, K. S., Witt, H. T., and Saenger, W. 1993. Three dimensional structure of system I of photosynthesis at 6 Å resolution. *Nature* 361:326–331.

Liebl, U., Mockensturm-Wilson, M., Trost, J. T., Brune, D. C., Blankenship, R. E., and Vermaas, W. F. J. 1993. Single core polypeptide in the reaction center of the photosynthetic bacterium *Heliobacillus mobilis*: Structural implications and relations to other photosystems. *Proc. Natl. Acad. Sci. (USA)* 90:7124–7128.

Madigan, M. T. 1992. The family Heliobacteriaceae. *In* The Prokaryotes. 2nd A. Balows, H. G. Trüper, M. Dworkin, K. H. Schliefer, and W. Harder, editors. Springer-Verlag, Berlin, 1982–1992.

Michel, H., and Deisenhofer, H. 1988. Relevance of the photosynthetic reaction center from purple bacteria to the structure of Photosystem II. *Biochemistry* 27:1–7.

Moore, J. W., and Pearson, R. G. 1981. Kinetics and Mechanism; A Study of Homogeneous Chemical Reactions, John Wiley and Sons, New York, 296–300.

Nitschke, W., Setif, P., Liebl, U., Feiler, U., and Rutherford, A. W. 1990a. Reaction center photochemistry of *Heliobacterium chlorum*. *Biochemistry* 29:11079–11088.

Nitschke, W., Feiler, U., and Rutherford, A. W. 1990b. Photosynthetic reaction center of green sulfur bacteria studied by EPR. *Biochemistry* 29: 3834–3842.

Nuijs, A. M., Van Dorssen, R. J., Duysens, L. N. M., and Amesz, J. 1985. Excited states and primary photochemical reactions in the photosynthetic bacterium *Heliobacterium chlorum*. *Proc. Natl. Acad. Sci. (USA)* 82: 6965–6968.

Otte, S. C. M., Kleinherenbrink, F. A. M., and Amesz, J. 1993. Energy transfer between the reaction center and the antenna in purple bacteria. *Biochim. Biophys. Acta* 1143:84–90.

Owens, T. G., Webb, S. P., Mets, L., Alberte, R. S., and Fleming, G. R. 1987. Antenna size dependence of the fluorescence decay in the core antenna of Photosystem I: Estimates of charge separation and energy transfer rates. *Proc. Natl. Acad. Sci. (USA)* 84:1532–1536.

Pearlstein, R. M. 1982. Exciton migration and trapping in photosynthesis. *Photochem. Photobiol.* 35:835–844.

Pearlstein, R. M. 1984. Photosynthetic exciton migration and trapping. *In* Advances in Photosynthesis Research. C. Sybesma, Editor. Martinus Nijhoff/Dr. W. Junk, The Hague, I:13–20.

Prince, R. C., and Olson, J. M. 1976. Some thermodynamic and kinetic properties of the primary photochemical reactants in a complex from a green photosynthetic bacterium. *Biochim. Biophys. Acta* 423:357–362.

Prince, R. C., Gest, H., and Blankenship, R. E. 1985. Thermodynamic properties of the photochemical reaction center of *Heliobacterium chlorum*. *Biochim. Biophys. Acta* 810:377–384.

Sètif, P. 1992. Energy transfer and trapping in Photosystem I. *In* The Photosystems: Structure, Function and Molecular Biology. J. Barber, editor. Elsevier, Amsterdam, 471:499.

Shuvalov, V. A., Nuijs, A. M., van Gorkom, H. J., Smit, H. W. J., and Duysens, L. M. N. 1986. Picosecond absorbance changes upon selective excitation of the primary electron donor P-700 in Photosystem I. *Biochim. Biophys. Acta* 850:319–323.

Smit, H. W. J., Van Dorssen, R. J., and Amesz, J. 1989. Charge separation and trapping efficiency in membranes of *Heliobacterium chlorum* at low temperature. *Biochim. Biophys. Acta* 973:212–219.

Sundström, V., and van Grondelle, R. 1990. Energy transfer in photosynthetic light-harvesting systems. *J. Opt. Soc. Am. [B]* 7:1595–1603.

Sundström, V., and van Grondelle, R. 1991. Dynamics of excitation energy transfer in photosynthetic bacteria. *In* Chlorophylls. H. Scheer, editor. CRC, Boca Raton, FL, 1097–1124.

Taguchi, A. K. W., Stocker, J. W., Alden, R. G., Causgrove, T. P., Peloquin, J. M., Boxer, S. G., and Woodbury, N. W. 1992. Biochemical characterization and electron-transfer reactions of sym1, a *Rhodobacter capsulatus* reaction center symmetry mutant which affects the initial electron donor. *Biochemistry* 31:10345–10355.

Trissl, H. W. 1993. Long-wavelength absorbing antenna pigments and heterogeneous absorption bands concentrate excitons and increase absorption cross section. *Photosynth. Res.* 35:247–263.

Trissl, H. W., Hecks, B., and Wulf, K. 1993. Invariable trapping times in photosystem I upon excitation of minor long-wavelength-absorbing pigments. *Photochem. Photobiol.* 57:108–112.

Trost, J. T., and Blankenship, R. E. 1989. Isolation of a photoactive photosynthetic reaction center core antenna complex from *Heliobacillus mobilis*. *Biochemistry* 28:9898–9904.

Trost, J. T., Brune, D. C., and Blankenship, R. E. 1992. Protein sequences and redox titrations indicate that the electron acceptors in reaction centers from heliobacteria are similar to Photosystem I. *Photosynth. Res.* 32: 11–22.

Turconi, S., Schweitzer, G., and Holzwarth, A. R. 1993. Temperature dependence of picosecond fluorescence kinetics of a cyanobacterial photosystem I particle. *Photochem. Photobiol.* 57:113–119.

Van de Meent, E. J., Kleinherenbrink, F. A. M., and Amesz, J. 1990. Purification and properties of an antenna-reaction center complex from heliobacteria. *Biochim. Biophys. Acta* 1015:223–230.

Van de Meent, E. J., Kobayashi, M., Erkelens, C., Van Veelen, P. A., Amesz, J., and Watanabe, T. 1991. Identification of 8(1)-hydroxychlorophyll*a* As

a functional reaction center pigment in heliobacteria. *Biochim. Biophys. Acta* 1058:356–362.

Van Dorssen, R. J., Vasmel, H., and Amesz, J. 1985. Antenna organization and energy transfer in membranes of *Heliobacterium chlorum*. *Biochim. Biophys. Acta* 809:199–203.

Van Kan, P. J. M., Aartsma, T. J., and Amesz, J. 1989. Primary photosynthetic processes in *Heliobacterium chlorum* at 15 K. *Photosynth. Res.* 22:61–68.

Van Noort, P. I., Gormin, D. A., Aartsma, T. J., and Amesz, J. 1992. Energy transfer and primary charge separation in *Heliobacterium chlorum* studied by picosecond time-resolved transient absorption spectroscopy. *Biochim. Biophys. Acta* 1140:15–21.

Vos, M. H., Klaassen, H. E., and Van Gorkom, H. J. 1989. Electron transport in *Heliobacterium chlorum* whole cells studied by electroluminescence and absorbance difference spectroscopy. *Biochim. Biophys. Acta* 973: 163–169.